CHEMISTRY
A EUROPEAN JOURNAL

DOI: 10.1002/chem.200900945

Total Synthesis, Characterization, and Conformational Analysis of the Naturally Occurring Hexadecapeptide Integramide A and a Diastereomer

Marta De Zotti,[a] Francesca Damato,[a] Fernando Formaggio,[a] Marco Crisma,[a] Elisabetta Schievano,[a] Stefano Mammi,[a] Bernard Kaptein,[b] Quirinus B. Broxterman,[b] Peter J. Felock,[c] Daria J. Hazuda,[c] Sheo B. Singh,[c] Jochen Kirschbaum,[d] Hans Brückner,[d] and Claudio Toniolo*[a]

Dedicated to the Centenary of the Italian Chemical Society and to the memory of Professor Ernesto Scoffone, founder of peptide chemistry in Italy and a great mentor

Abstract: Integramide A is a 16-amino acid peptide inhibitor of the enzyme HIV-1 integrase. We have recently reported that the absolute stereochemistries of the dipeptide sequence near the C terminus are L-Iva^{14}-D-Iva^{15}. Herein, we describe the syntheses of the natural compound and its D-Iva^{14}-L-Iva^{15} diastereomer, and the results of their chromatographic/mass spectrometric analyses. We present the conformational analysis of the two compounds and some of their synthetic intermediates of different main-chain length in the crystal state (by X-ray diffraction) and in solvents of different polarities (using circular dichroism, FTIR absorption, and 2D NMR techniques). These data shed light on the mechanism of inhibition of HIV-1 integrase, which is an important target for anti-HIV therapy.

Keywords: circular dichroism · IR spectroscopy · NMR spectroscopy · peptides · X-ray diffraction

Introduction

Like all retroviruses, human immunodeficiency virus type 1 (HIV-1) depends upon the integration of a DNA copy of its viral genome into the host cell chromosomes as part of its infection cycle. Several steps in this integration process are catalyzed by the enzyme HIV-1 integrase. The integration of HIV-1 DNA into the host chromosome is achieved by the integrase protein performing a series of DNA cutting and joining reactions.

Integrase is an attractive target for anti-HIV therapy because it is essential for virus replication and, unlike protease and reverse transcriptase, there are no known counterparts in the host cell. Furthermore, integrase takes advantage of a single active site to accommodate two different conformations of DNA substrates, which may constrain the ability of HIV to develop drug resistance to integrase inhibitors.[1] Several classes of HIV-integrase inhibitors are known,[2] including some non-α-aminoisobutyric acid (Aib)/isovaline (Iva) peptides.[3] However, a recent publication from three of the authors of this paper has dealt with two naturally occurring, nonribosomal peptide molecules (integramides A and B) that exhibit significant inhibitory activities.[4]

Integramides are linear peptides, 16 amino acids long and rich in Aib and Iva residues. There are four Aib and five Iva residues in the sequence of integramide A, and three Aib and six Iva residues in integramide B; integramide A has an Aib residue at position 8, whereas its B analogue has an L-

[a] Dr. M. De Zotti, F. Damato, Prof. F. Formaggio, Dr. M. Crisma, Dr. E. Schievano, Prof. S. Mammi, Prof. C. Toniolo
Institute of Biomolecular Chemistry, CNR, Padova Unit
Department of Chemistry University of Padova
via Marzolo 1, 35131 Padova (Italy)
Fax: (+39) 049-827-5239
E-mail: claudio.toniolo@unipd.it

[b] Dr. B. Kaptein, Dr. Q. B. Broxterman
DSM Pharmaceutical Products
Innovative Synthesis and Catalysis
P.O. Box 18, 6160 MD Geleen (The Netherlands)

[c] Dr. P. J. Felock, Dr. D. J. Hazuda, Dr. S. B. Singh
Merck Research Laboratories, Rahway
NJ 07065 and West Point, PA 19486 (USA)

[d] Dr. J. Kirschbaum, Prof. H. Brückner
Department of Food Sciences
Interdisciplinary Research Centre for Biosystems
Land Use and Nutrition, University of Giessen
35392 Giessen (Germany)

Supporting information for this article is available on the WWW under http://dx.doi.org/10.1002/chem.200900945.

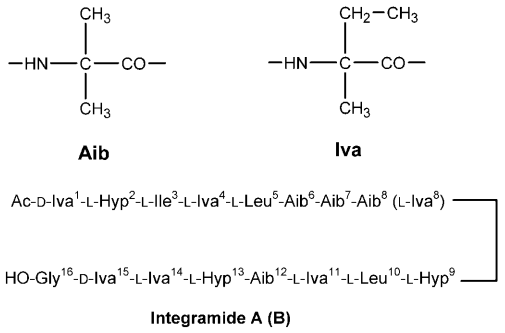

Iva residue in this position. In both integramides A and B, the C terminus is free and the N terminus is acetylated (Ac). In the initial work,[4] the stereochemical configuration of the two consecutive C-terminal Iva^{14}-Iva^{15} residues could not be determined, although it was known that one is L and the other is D. More recently, using HPLC and NMR techniques and the two L-Iva^{14}-D-Iva^{15} and D-Iva^{14}-L-Iva^{15} synthetic diastereomeric hexadecapeptides, we were able to elucidate this originally unresolved stereochemical problem, providing unambiguous evidence that the natural inhibitors contain the L-Iva^{14}-D-Iva^{15} chiral pair.[5] We also showed that the stereochemical inversion in the Iva^{14}- Iva^{15} natural sequence is in general not detrimental and might be even slightly beneficial for activity against the strand-transfer reaction.

Herein, we describe in detail the strategy we exploited in solution for the challenging syntheses of the two diastereomeric hexadecapeptides, and their extensive characterization using HPLC, chiral chromatography, and mass spectrometry. In addition, the results of an in-depth conformational investigation of the two hexadecapeptides and some of their short-sequence synthetic intermediates using X-ray diffraction, CD, FTIR absorption, and NMR techniques are presented. In our previous communication on these compounds,[5] only the results of the configurational study were reported; neither the synthetic approach and the related analytical data nor the conformational findings were discussed. A preliminary NMR spectroscopic conformational investigation of integramide A was already published,[4] but, as opposed to the helix-supporting solvent used in this work (deuterated 2,2,2-trifluoroethanol, [D_2]TFE), the previous work was performed in deuterated pyridine, which is not entirely appropriate for such an analysis because of its known tendency to interact with the hydrogen-bonding donor (peptide) NH groups.

Results and Discussion

Synthesis and characterization: For the large-scale production of enantiomerically pure L-Iva and D-Iva, an economically attractive and generally applicable chemoenzymatic synthesis developed by DSM was used.[6] The method involves a combination of organic synthesis for the preparation of the racemic α-amino amides, followed by optical resolution using a broadly specific α-amino amidase.

The segment condensation strategy adopted for the synthesis of the two diastereomeric (L-Iva^{14}-D-Iva^{15} and D-Iva^{14}-L-Iva^{15}) hexadecapeptides in solution is illustrated in Scheme 1. The three planned segments **B**, **C**, and **D** are of similar length. The synthesis avoids Aib(Iva)-Hyp dipeptide sequences (Hyp = (2*S*,4*R*)-4-hydroxyproline), which are acid labile and prone to undergo intramolecular cyclization to 2,5-dioxopiperazine when located at the N terminus. In addition, epimerization in the coupling reaction is prevented due to the absence of chiral C^{α}-trisubstituted amino acids in the last and penultimate positions of the chain.[7] Indeed, any C activation of amino acid derivatives and peptide segments, such as **A**, **B**, and **C**, with a C-terminal C^{α}-tetrasubstituted amino acid (Iva or Aib), is known to produce an otherwise easily epimerizable 5(4*H*)-oxazolone intermediate to a considerable extent.

For the formation of the difficult peptide bonds, in particular those connecting either two sterically demanding C^{α}-tetrasubstituted amino acids (Aib/Iva) or one of these amino acids followed by an N-alkylated Hyp residue,[7] the carboxyl group of the N^{α}-protected amino acid or peptide was activated with the *N*-ethyl-*N*′-(3-dimethylaminopropyl)-carbodiimide (EDC)/7-aza-1-hydroxy-1,2,3-benzotriazole (HOAt) method.[8] The poorly reactive secondary alcohol functionalities in the side chains of the Hyp residues were used without protection. The C-terminal O*t*Bu carboxylic ester protection was removed by the classical trifluoroacetic acid method in segments **B** and **C**, which lack any Aib(Iva)–Hyp bond, whereas a mildly acidic fluoroalcohol (1,1,1,3,3,3-hexafluoroacetone hydrate) was used to afford the final **A–B–C–D** hexadecapeptide.[9]

The HPLC profiles shown in Figure 1 demonstrate the purity of the two Ac/OH hexadecapeptide diastereomers. As reported in ref. [5], the chromatographic behavior of natural integramide A is identical to that of the L-Iva^{14}-D-Iva^{15} diastereomer, but differs significantly from that of the D-Iva^{14}-L-Iva^{15} diastereomer.

A total acid hydrolyzate of each of the two synthetic hexadecapeptide diastereomers was derivatized with Marfey's reagent according to the literature procedure.[10] The L-Iva

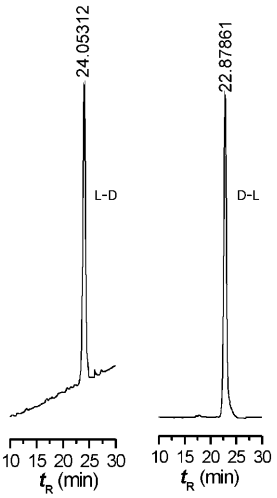

Figure 1. HPLC profiles for the two synthetic hexadecapeptide diastereomers L-Iva^{14}-D-Iva^{15} (**L- D**) and D-Iva^{14}-L-Iva^{15} (**D-L**). Conditions: analytical Phenomenex Kromasil C_{18} column (particle size: 5 μm; pore size: 100 Å); gradient system: 65% to 80% B in 30 min; eluant A, 9:1 0.05% aqueous trifluoroacetic acid (TFA)/CH_3CN; eluant B: 9:1 CH_3CN/ 0.05% aqueous TFA; flow rate: 1 mL min^{-1}; room temperature; absorbance detector at 226 nm.

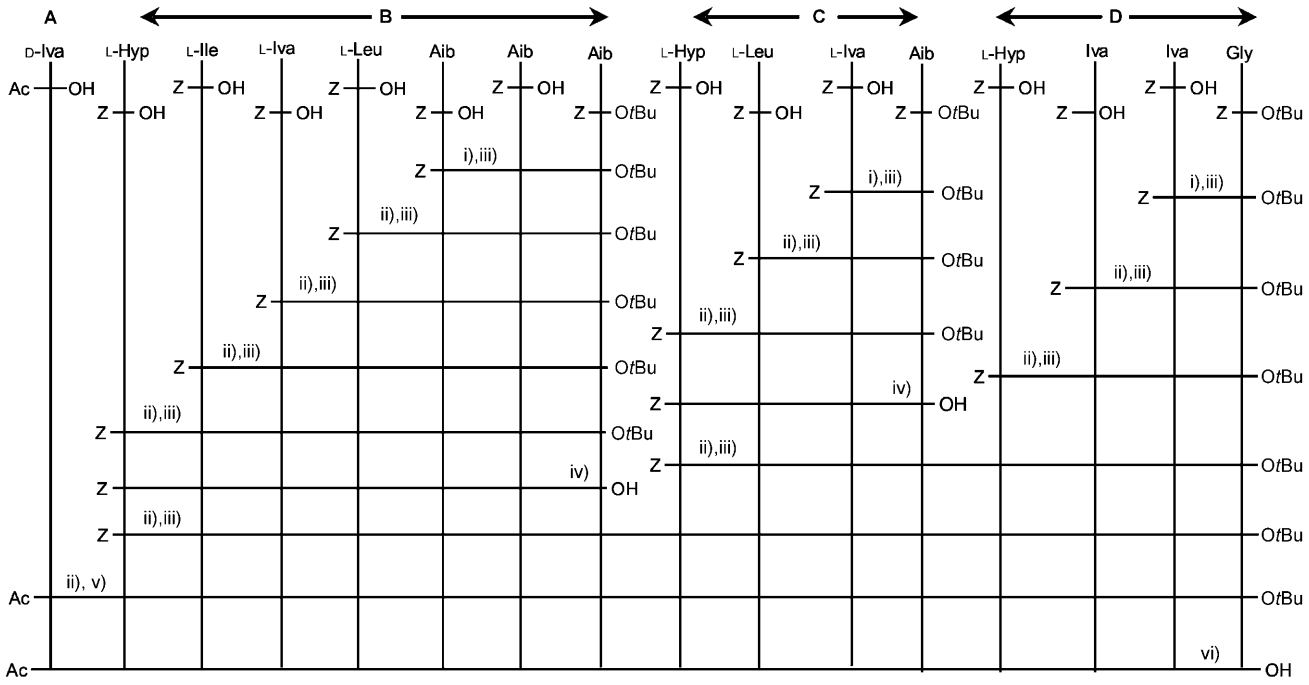

Scheme 1. Strategy adopted for the synthesis of the two hexadecapeptide diastereomers Ac/OH **A–B–C–D**[Hyp^{2,9,13}], (-D-Iva^{14}-L-Iva^{15}-) and (-L-Iva^{14}-D-Iva^{15}-). i) H_2/Pd in distilled CH_2Cl_2; ii) H_2/Pd in MeOH; iii) EDC and HOAt (1.3 equiv each) in distilled CH_2Cl_2, keeping the pH at 8 by adding *N*-methylmorpholine (NMM); iv) trifluoroacetic acid (10 equiv) in CH_2Cl_2; v) EDC, HOAt, and Ac-D-Iva-OH (15 equiv each) in *N*,*N*-dimethylformamide (DMF), keeping the pH at 8 by adding NMM; vi) 1,1,1,3,3,3-hexafluoroacetone hydrate. (EDC, *N*-ethyl-*N*′-(3-dimethylaminopropyl)carbodiimide, HOAt, 7-aza-1-hydroxy-1,2,3-benzotriazole).

(eluted at 27.9 min) and D-Iva (eluted at 30.3 min) enantiomers were baseline resolved by HPLC. The average L-Iva/D-Iva ratio obtained (two analyses for each sample) was 1.48 (±0.03) for the L-Iva^{14}-D-Iva^{15} hexadecapeptide and 1.43 (±0.03) for the D-Iva^{14}-L-Iva^{15} hexadecapeptide.[4] These two experimental values should be compared with the calculated ratio (3 L-Iva and 2 D-Iva) of 1.50. A synthetic, racemic D,L-Iva amino acid, used as a standard, gave the expected L/D ratio (1.00).

Total acid hydrolyzates of natural integramide A and the synthetic L-Iva^{14}-D-Iva^{15} hexadecapeptide were separately converted into N$^{\alpha}$-trifluoroacetylamino 2-propyl esters. The resulting derivatives were resolved on a Chirasil-L-Val capillary column and analyzed by selected-ion monitoring (SIM) mass spectrometry. The presence of Aib, Gly, L-Leu, L-Ile, and L-Hyp was detected. Moreover, the derivatives of L-Iva and D-Iva, satisfactorily resolved, provided L-Iva/D-Iva ratios of 1.48 (natural compound) and 1.42 (synthetic compound). Trace amounts of D-Leu in the natural compound (1.8%) and in the synthetic compound (3.8%) are attributed to minor sequence-dependent racemization during acid hydrolysis and epimerization during the coupling steps in the peptide synthesis.

The electrospray ionization collision-induced dissociation (ESI-CID) mass spectrum of the synthetic L-Iva^{14}-D-Iva^{15} hexadecapeptide (Figure 2) shows the intense peak of the sodium adduct of the molecular ion (*m*/*z* 1653.9), as well as a regular series of b_3–b_8 acylium ions (*m*/*z* 368.0, 467.0, 580.0, 665.2, 750.2, and 835.3), resulting from the sequence [Ac-Iva-Hyp-Ile^3-Iva-Leu-Aib-Aib-Aib^8]$^+$. Ions b_{11} and b_{14} (*m*/*z* 1160.3 and 1457.3, respectively) are of very low abundance, whereas ions b_{12} and b_{15} (*m*/*z* 1245.3 and 1556.3, respectively) are remarkably intense. The high intensity of the b_8 and b_{12} ions is related to the preferred cleavage of the Aib^8–Hyp^9 and Aib^{12}–Hyp^{13} peptide bonds.[10] In the CID-off mode, the fragment ions b_9, b_{10}, and b_{13} are not generated (but they are formed when CID 50% is applied, not shown). The a_2 fragment ion (*m*/*z* 226.9) results from loss of CO from the b_2 ion. An ion denoted x_4 at *m*/*z* 411.0 represents the protonated internal tetrapeptide fragment ion Hyp^9-Leu-Iva-Aib^{12}. Loss of the C-terminal Aib is therefore assumed to generate the ion at *m*/*z* 326.0. The ESI-CID mass spectrum of the synthetic L-Iva^{14}-D-Iva^{15} hexadecapeptide (Figure 2) and that of natural integramide A show almost perfect agreement.

Crystal-state conformational analysis: Despite a number of attempts, we were unable to grow a single crystal from either of the two hexadecapeptide diastereomers. However, we succeeded in preparing crystals suitable for X-ray diffraction from four terminally protected segments of integramide A or its D-Iva-L-Iva diastereomer: 1) Z-D-Iva-L-Iva-Gly-O*t*Bu (Z = benzyloxycarbonyl; O*t*Bu = *tert*-butoxy), the C-terminal tripeptide of segment **D**, already described in ref. [11]; 2) Z-L-Hyp-L-Iva-D-Iva-Gly-O*t*Bu, a tetrapeptide that spans the full sequence of segment **D**; 3) Z-L-Iva-L-Leu-(Aib)$_3$-O*t*Bu; and 4) Z-L-Ile-L-Iva-L-Leu-(Aib)$_3$-O*t*Bu, the C-terminal penta- and hexapeptides of segment **B**. The

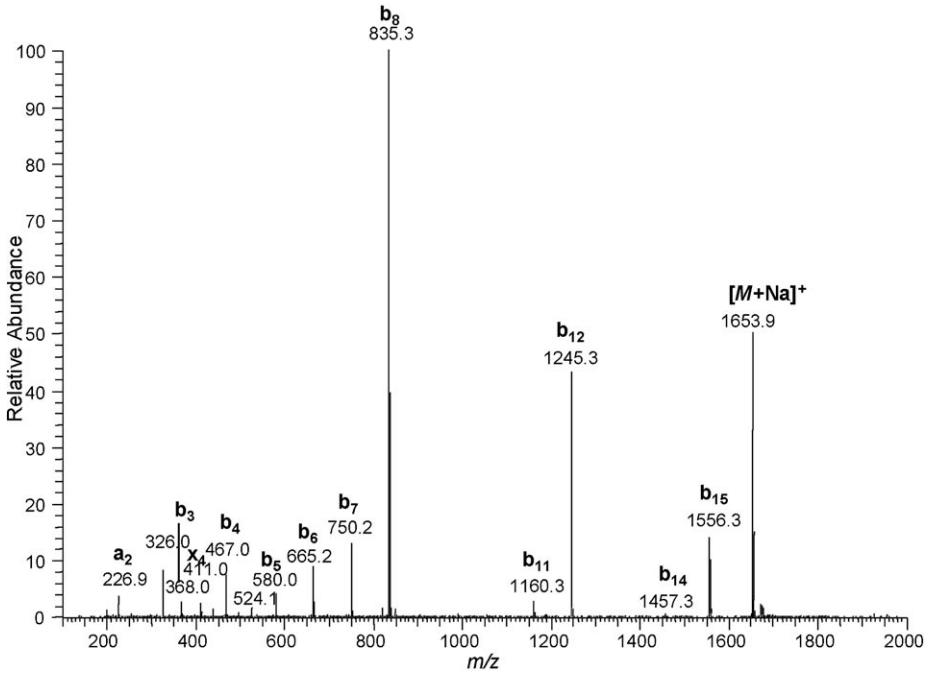

Figure 2. Positive ion ESI-MS for the synthetic L-Iva[14]-D-Iva[15] hexadecapeptide.

molecular structures of the last three peptides are illustrated in Figures 3, 4, and 5. Their backbone torsion angles are listed in Table 1.

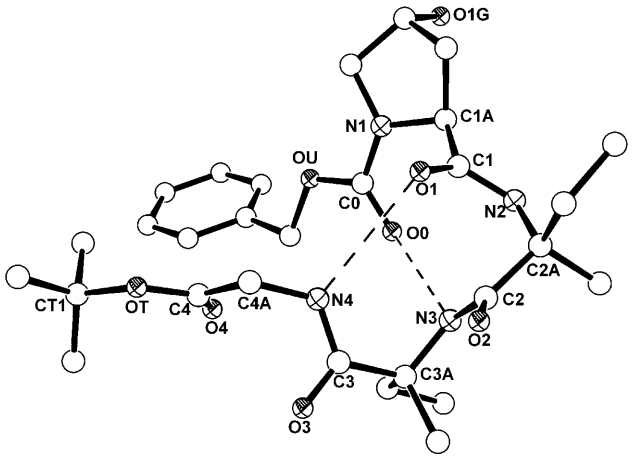

Figure 3. X-ray diffraction structure of Z-L-Hyp-L-Iva-D-Iva-Gly-O*t*Bu with atom numbering. Hydrogen atoms were omitted for clarity. Dashed lines represent intramolecular C=O···H–N hydrogen bonds.

Table 1. Backbone torsion angles [°] for the peptides studied in this work

Torsion angle	Z-L-Hyp-L-Iva-D-Iva-Gly-O*t*Bu	Z-L-Iva-L-Leu-(Aib)$_3$-O*t*Bu	Z-L-Ile-L-Iva-L-Leu-(Aib)$_3$-O*t*Bu
ω_0	−170.2(4)	−177.6(8)	−165.6(8)
ϕ_1	−56.4(5)	−58.4(11)	−62.3(11)
ψ_1	132.5(4)	−23.3(11)	−48.0(11)
ω_1	173.0(3)	178.0(8)	−173.1(7)
ϕ_2	55.3(5)	−64.6(10)	−56.2(11)
ψ_2	39.2(5)	−10.9(11)	−30.8(12)
ω_2	169.4(4)	173.2(8)	−175.3(8)
ϕ_3	72.8(6)	−54.9(10)	−58.8(11)
ψ_3	28.2(7)	−33.8(10)	−28.1(12)
ω_3	171.2(5)	−176.1(7)	179.3(8)
ϕ_4	−79.3(8)	−73.5(10)	−53.4(11)
ψ_4	171.6(5)[a]	−7.4(10)	−33.5(10)
ω_4	178.0(5)[b]	−167.7(8)	−173.8(7)
ϕ_5	–	50.9(11)	−59.1(11)
ψ_5	–	43.3(12)[c]	−37.8(12)
ω_5	–	174.8(10)[d]	−164.1(9)
ϕ_6	–	–	46.4(13)
ψ_6	–	–	48.5(11)[e]
ω_6	–	–	171.1(10)[f]

[a] N4-C4A-C4-OT. [b] C4A-C4-OT-CT1. [c] N5-C5A-C5-OT. [d] C5A-C5-OT-CT1. [e] N6-C6A-C6-OT. [f] C6A-C6-OT-CT1.

In the structure of the tetrapeptide (Figure 3), two C=O···H–N intramolecular hydrogen bonds are seen between the peptide N3–H and urethane C0=O0 groups and between the peptide N4–H and peptide C1=O1 groups. Both hydrogen bonds are weak[12] (Table S1 in the Supporting Information). The N-terminal-L-Hyp-L-Iva β-turn structure[13] is nonhelical type II, whereas the next one (-L-Iva-D-Iva-) is helical type III′. Both Iva residues, independent of their configuration, adopt ϕ,ψ torsion angles falling in the left-handed helical region of the Ramachandran map. Two intermolecular hydrogen bonds involve the peptide N2–H and side-chain Hyp hydroxyl groups as donors, and the peptide C2=O2 and C1=O1 as acceptors, respectively. The -D-Iva-L-Iva- sequence in the tripeptide Z-D-Iva-L-Iva-Gly-O*t*Bu, shorter by one residue at the N terminus, is also helical.[11] The structure of the strictly related tetrapeptide Z-L-Pro-L-Iva-D-Iva-Gly-O*t*Bu also shows a nonhelical conformation, with two consecutive β-turns of type II, III′.[11] These findings are in line with the well-known structural bias of the L-Pro/L-Hyp residues for a *semi*-extended (or poly-(Pro)$_n$ II) conformation[14] and of the Iva helical screw-sense indifference, due to the small variation in length between its two side chains.[15]

The pentapeptide molecule (Figure 4), particularly rich in helicogenic Aib residues,[16] is highly folded. The L-Iva-L-Leu-Aib-Aib segment is stabilized by three consecutive C=O···H–N intramolecular hydrogen bonds (C0=O0···H–N3, C1=O1···H–N4, C2=O2···H–N5), generating a full turn of a 3_{10}-helix.[17] However, this right-handed structure is not regu-

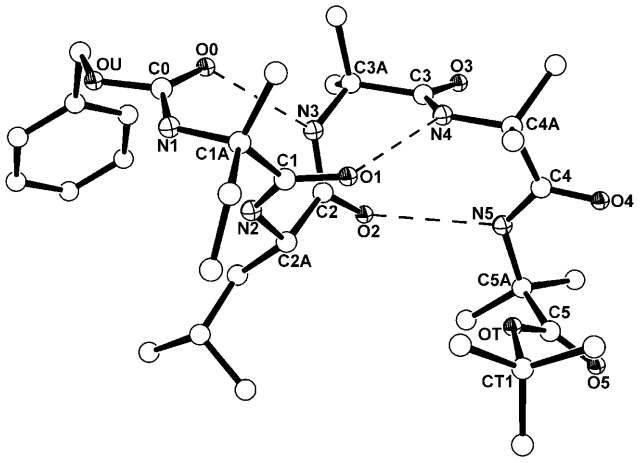

Figure 4. X-ray diffraction structure of Z-L-Iva-L-Leu-(Aib)$_3$-O*t*Bu with atom numbering. Only the major occupancy site of the L-Iva C$^{\gamma}$ atom is shown. Hydrogen atoms were omitted for clarity. Dashed lines represent intramolecular C=O···H–N hydrogen bonds.

lar, in particular at the level of the L-Leu^2 and Aib^4 residues, in which the corresponding ψ torsion angles are well below the typical −30° value, generating type I instead of type III β-turns. Nonetheless, the intramolecular hydrogen bonds exhibit normal N···O distances and N–H···O angles. The typical screw-sense inversion with respect to the preceding residues in the backbone, usually observed at the C terminus of a 3_{10}-helical peptide for a C$^{\alpha}$-tetrasubstituted α-amino ester,[16] is also noted in this compound. The pentapeptide molecules are held together head-to-tail through a C4=O4···H–N1 intermolecular hydrogen bond.

At partial variance with its pentapeptide synthetic precursor, the hexapeptide (Figure 5) adopts a regular, right-handed, 3_{10}-helical structure in the crystalline state (Table 1). Four consecutive, type III β-turns are observed, each stabilized by a C=O···H–N intramolecular hydrogen bond. The hydrogen bonds involve the N3–H, N4–H, N5–H, and N6–H groups as donors and the C0=O0, C1=O1, C2=O2, and C3=O3 groups as acceptors, respectively. Only the N-terminal hydrogen bond is rather weak. Also in this compound, we observe a screw-sense inversion for the C-terminal, helical Aib residue. Two intermolecular hydrogen bonds (C4=O4···H–N1 and C5=O5···H-N2), the latter quite weak, stabilize the head-to-tail packing mode of the helical molecules in the crystal.

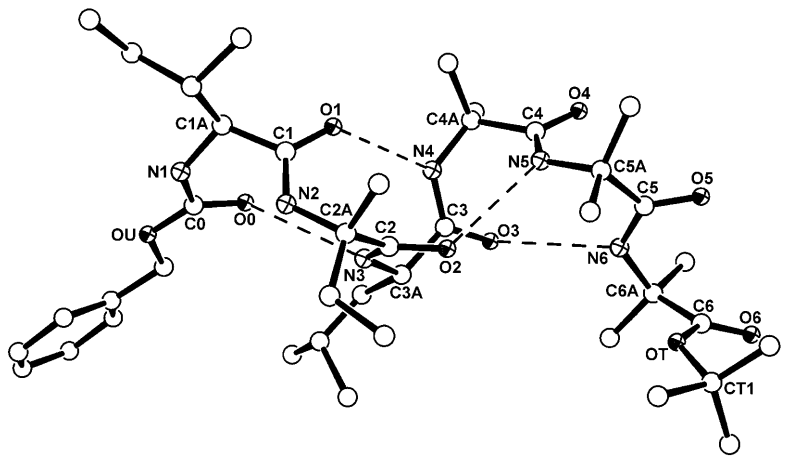

Figure 5. X-ray diffraction structure of Z-L-Ile-L-Iva-L-Leu-(Aib)$_3$-O*t*Bu acetonitrile hemisolvate with atom numbering. Hydrogen atoms were omitted for clarity. Dashed lines represent intramolecular C=O···H–N hydrogen bonds.

From this crystal-state conformational analysis, it seems reasonable to conclude that most of the N-terminal heptapeptide segment **B** of integramide A possesses a strong propensity for a regular, right-handed, 3_{10}-helical structure. On the other hand, the C-terminal segment **D** is not helical as such, most probably because of the presence of a Janus-headed Hyp residue located at position 1. However, it would not be surprising to see this segment as well in a regular folded conformation when incorporated at the C terminus of a pre-existing helical stretch.

Solution conformational analysis: We investigated the conformational preferences in solution for the two hexadecapeptide diastereomers (L-Iva^{14}-D-Iva^{15} and D-Iva^{14}-L-Iva^{15}) and for natural integramide A under different solvent and temperature conditions by means of CD, FTIR absorption and 2D-NMR spectroscopic techniques.

The CD spectra of the two synthetic compounds in MeOH, 2,2,2,-trifluoroethanol (TFE), and a 100 mM aqueous solution of sodium dodecylsulfate (SDS) are shown in Figure 6. In Figure 7, the two curves in TFE are compared with that of natural integramide A in the same fluoroalcohol. By changing the solvent, no dramatic alterations are seen in the CD patterns, which highlights the remarkable secondary structure stability of the two compounds. This conclusion is corroborated by the absence of any variation in the spectra by heating from 5 to 55 °C in MeOH (not shown). The shapes of the CD patterns clearly indicate that both compounds fold in a right-handed helical structure of the mixed 3_{10}-/α-type (in MeOH, the 3_{10}-helix seems to prevail, whereas in SDS the α helix tends to be more populated). This information was extracted from the occurrence of two negative maxima near 205 and 225 nm and one positive maximum at about 195 nm, and from the ellipticity ratio $[\Theta]_R^{225}/[\Theta]_R^{205}$, which is known to be less than 0.50 for a high population of 3_{10}-helix and more than 0.60 for a high population of α helix.[18] In general, the highest ellipticity and, as a consequence, the most significant percentage of α helix is seen in

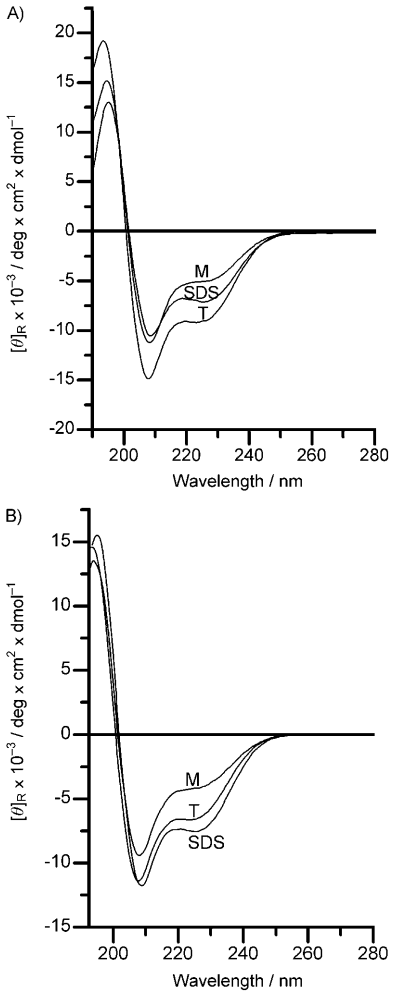

Figure 6. CD spectra for the two synthetic hexadecapeptide diastereomers L-Iva^{14}-D-Iva^{15} (**A**) and D-Iva^{14}-L-Iva^{15} (**B**) in MeOH (M), TFE (T), and a 100 mM aqueous solution of SDS. Peptide concentration: 1 mM.

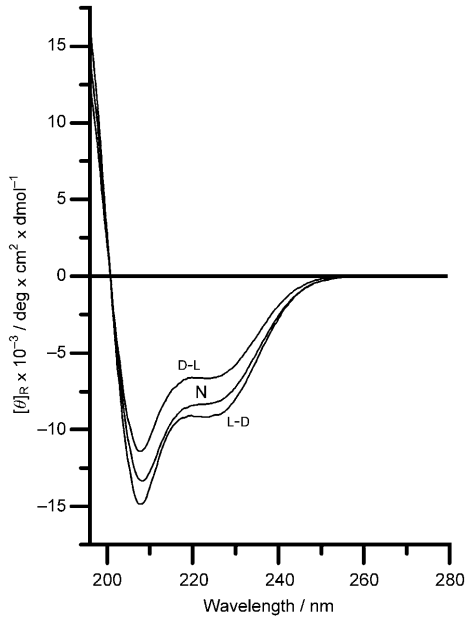

Figure 7. CD spectra for the two synthetic hexadecapeptide diastereomers L-Iva^{14}-D-Iva^{15} (**L-D**) and D-Iva^{14}-L-Iva^{15} (**D-L**), and natural integramide A (**N**) in TFE. Peptide concentration: 1 mM.

the structure-supporting solvent TFE[19] for both compounds. The CD patterns of the two hexadecapeptide diastereomers are similar to each other and to that of natural integramide A, suggesting that the chirality inversion in the Iva^{14}-Iva^{15} dipeptide segment does not induce any significant change in the overall secondary structure of the peptide. However, only the CD curve of the L-Iva^{14}-D-Iva^{15} peptide matches almost perfectly that of natural integramide A. Finally, the CD curves of the Z/O*t*Bu protected pentadecapeptides and of the Ac/O*t*Bu-protected hexadecapeptide synthetic precursors (not shown) nearly overlap with those of the two final diastereomeric compounds, showing that the observed 3_{10}-/α-helical conformation is already attained at the pentadecapeptide level and also before removal of the O*t*Bu C-terminal protecting group.

Figure 8 reports the conformationally informative N–H stretching region of the FTIR absorption spectra of the short, Z/O*t*Bu-protected segments **B**, **C,** and **D** (the latter for the L-Iva^{14}-D-Iva^{15} diastereomer) in $CDCl_3$ at two concentrations. The curves change only slightly on changing from concentrations of 1.0 to 0.1 mM (except for segment **C**, but only below 3320 cm^{-1}). This finding suggests that almost all observed C=O···H–N hydrogen bonding is intramolecular. The ratio between the areas of the band at 3350 cm^{-1} (associated with hydrogen-bonded NH groups[20]) and the band(s) above 3400 cm^{-1} (associated with free, solvated NH groups) is much lower for segment **C**, indicating that the latter peptide exhibits a remarkably reduced tendency to fold, probably related not only to its short main-chain length, but to its specific sequence as well, because it lacks any helicogenic C$^{\alpha}$-methylated α-amino acid in the N-terminal doublet. This structural information agrees with that found from the X-ray diffraction analysis described above. Consistent with this result, in the two longer segments **C–D** and **B–C–D** (spectra not shown), and in the two Ac/O*t*Bu-protected hexadecapeptide diastereomers (Figure 8), all containing the **C** segment, we found that the band at 3350 cm^{-1} is significantly broadened, which implies some conformational heterogeneity in this part of the molecule. Because the FTIR spectra of the two hexadecapeptide diastereomers are very similar, this spectroscopic technique does not allow any specific assignment. In these two FTIR spectra, the extremely weak band above 3400 cm^{-1} is indicative of the occurrence of highly folded species. At concentrations above 1.0 mM, the curves of all Z-protected synthetic intermediates do not suggest the onset of any significant amount of self-aggregated species, in contrast with those of the two Ac-blocked hexadecapeptide diastereomers, which are strongly indicative of self-aggregation (spectra not shown). Unfortunately, we could not record the spectra of the two final, synthetic Ac/OH hexadecapeptides due to their very low solubilities in $CDCl_3$.

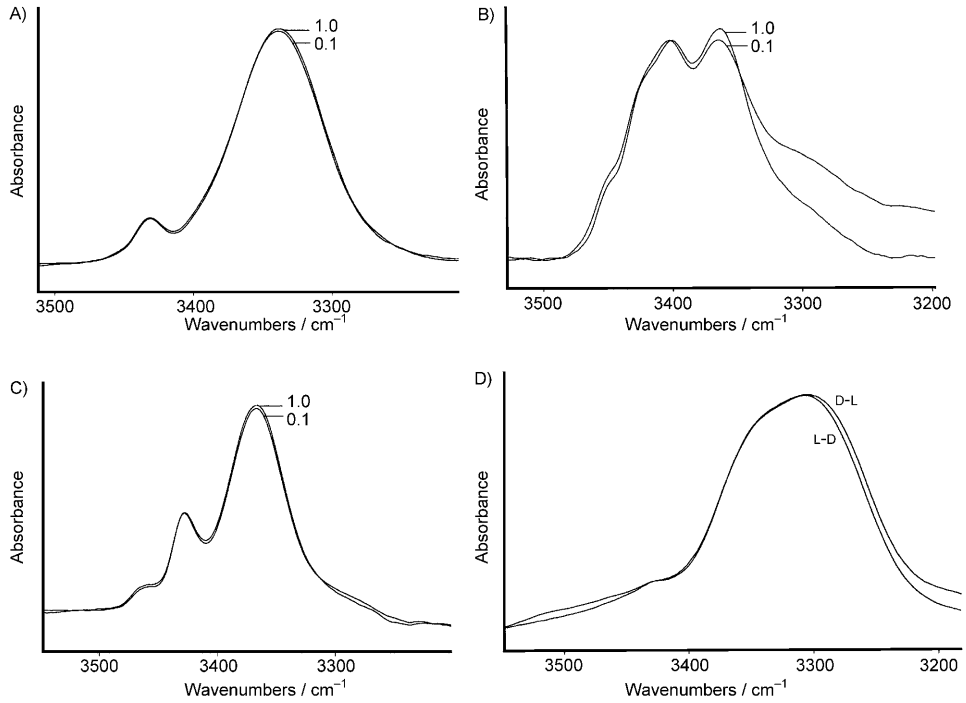

Figure 8. FTIR absorption spectra (N–H stretching region) of the Z/O*t*Bu protected segments **B** (A), **C** (B), and the L-Iva-D-Iva diastereomer of **D** (C) at the concentrations 1 mM (1.0) and 0.1 mM (0.1). D) The corresponding spectra for the two synthetic, Ac/O*t*Bu protected hexadecapeptide diastereomers L-Iva^{14}-D-Iva^{15} (**L-D**) and D-Iva^{14}-L-Iva^{15} (**D-L**) at 1 mM concentration. Solvent: $CDCl_3$.

bonds was detected. The 1D ^{1}H NMR spectrum does not show minor peaks and no sequential C$^\alpha$H–C$^\alpha$H NOESY cross-peaks were found. All NH–NH sequential connectivities are present, as well as some NH(*i*)–NH(*i*+2) connectivities. These results are consistent with a helical structure, which is not interrupted by the Hyp residues, as also confirmed by the presence in the NOESY spectrum of all of the connectivities between the Hyp C$^\delta$H protons and the NH proton of both the preceding and the following residues. A number of C$^\alpha$H(*i*)–NH(*i*+3), C$^\alpha$H(*i*)–NH(*i*+2), and C$^\alpha$H(*i*)–NH(*i*+4) cross peaks were observed. Together, these data support the presence of a mixed 3_{10}-/α-helical conformation.

The two methyl groups in the Aib residues belonging to chiral

A more detailed conformational characterization of integramide A was carried out by using 2D NMR spectroscopy. This study was performed in [D_2]TFE solution, in which the peptide exhibits a high propensity to fold into a helical structure as indicated by CD. The spin systems of the Gly, Leu, Hyp, and Ile residues were identified by using DQF-COSY and TOCSY spectra, whereas HMQC and HMBC experiments were used for the Aib and Iva residues. The sequential assignment was performed using NOESY spectra. Relevant regions of the NOESY spectrum at $\tau_m = 250$ ms are shown in Figures 9 and 10. The proton chemical shift assignment is reported in Table S2 in the Supporting Information. A summary of the NOE connectivities is shown in Figure 11.

Despite the presence of three Hyp residues, no trace of *cis* configuration at the Xxx–Hyp

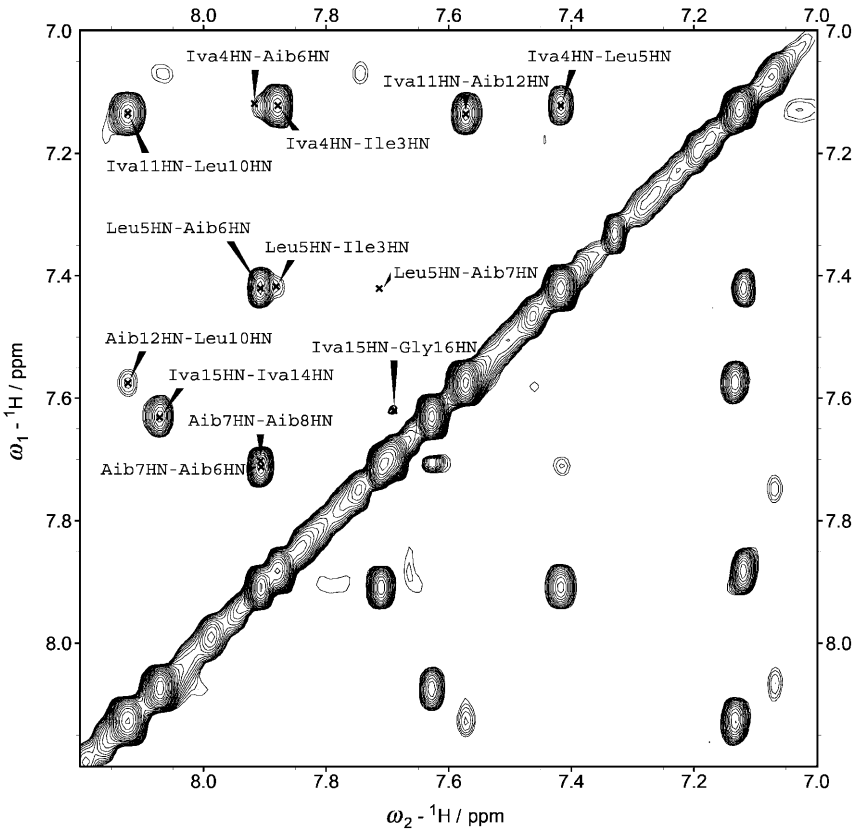

Figure 9. Amide region of the NOESY spectrum (600 MHz, $\tau_m = 250$ ms) of integramide A (1.45 mM in [D_2]TFE; 300 K). Medium-range ($i \rightarrow i+2$) interactions are marked.

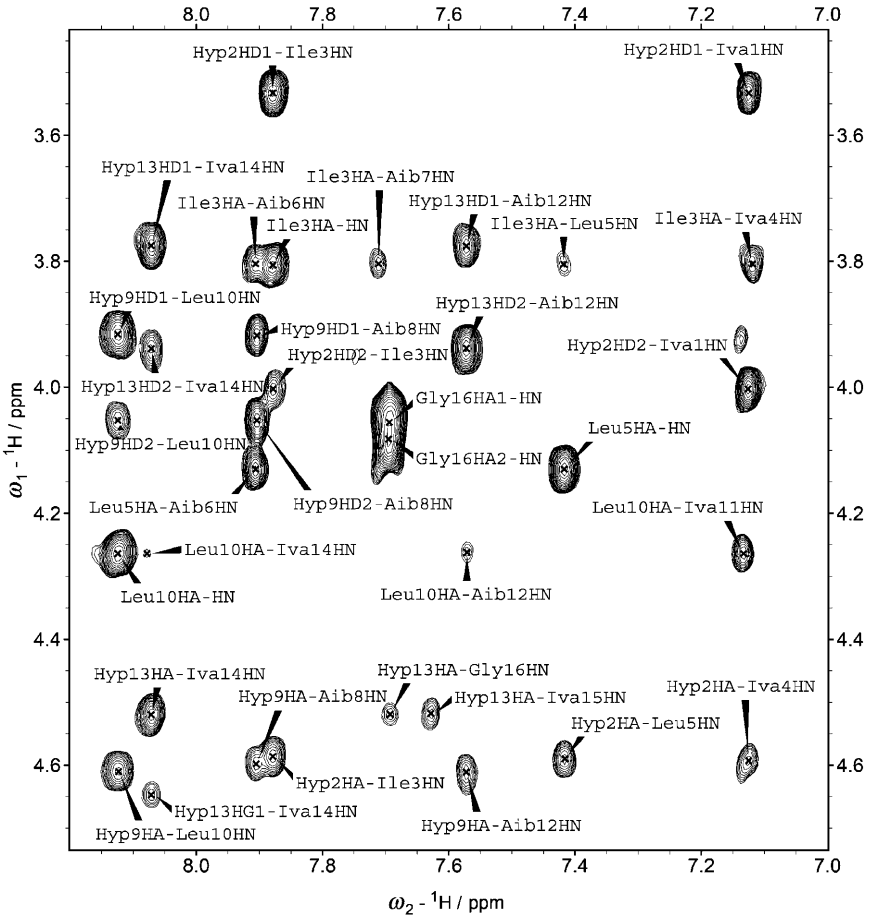

Figure 10. Fingerprint region of the NOESY spectrum (600 MHz, $\tau_m = 250$ ms) of integramide A (1.45 mM in [D_2]TFE; 300 K). Medium-range ($i \rightarrow i+2$, $i \rightarrow i+3$, and $i \rightarrow i+4$) interactions are marked.

peptides are diastereotopic. Consequently, the carbon atoms of the two methyl groups (labeled as β and β′) are expected to resonate at two different chemical shifts, above and below $\delta = 25$ ppm (Figure S1 in the Supporting Information). Jung et al.[21] have shown that the presence of a chiral center adjacent to two *gem*-methyl groups (as in an Aib residue) induces a chemical shift difference between these prochiral methyl carbons not higher than 0.5 ppm. However, if the observed difference in the ^{13}C NMR chemical shifts (termed chemical nonequivalence, CNE) of the two prochiral methyl carbons is 2 ppm or higher, this indicates the presence of a stable helical conformation. In Table S3 in the Supporting Information, the CNE values for the four Aib residues of integramide A are reported. All values are higher than 2 ppm, confirming the occurrence of a helical structure in TFE. The stereospecific assignment of the two diastereotopic

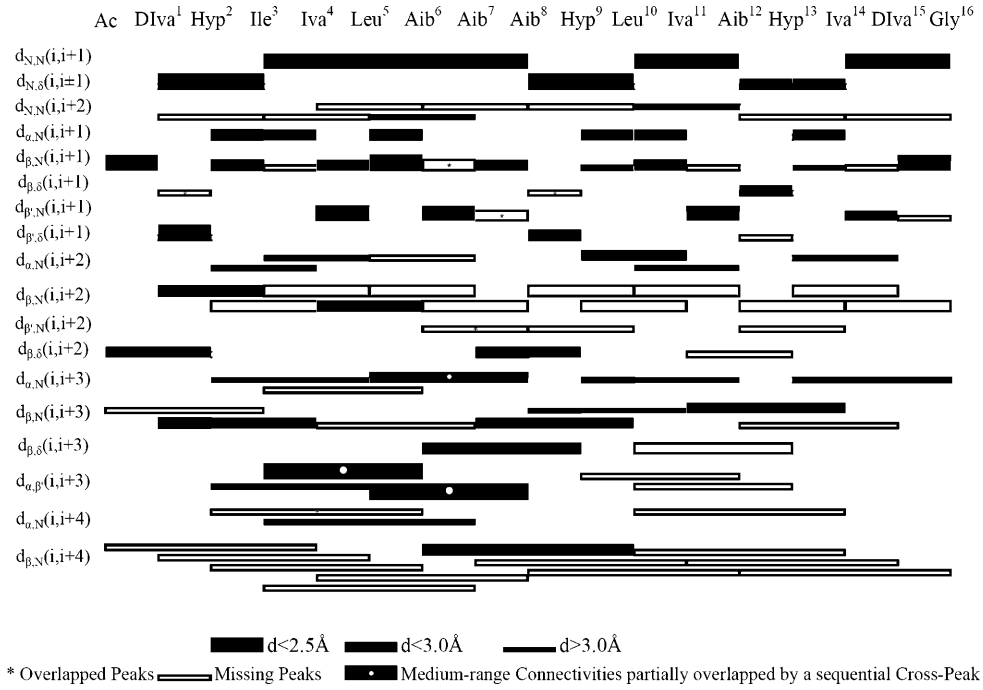

Figure 11. Summary of the NOESY connectivities for integramide A (1.45 mM in [D_2]TFE; 300 K). Peaks are grouped into three classes based upon their integrated volumes.

methyl groups was achieved through the C_β-selective HMQC spectrum, using the method reported by Bellanda et al.[22]

The conformational properties of integramide A were further investigated by distance geometry and restrained molecular dynamics (MD) calculations. A total of 99 interproton distance restraints were derived from the NOESY spectrum (Table 2) and used in the simulated annealing protocol.

Table 2. NOE constraints, deviations from idealized geometry, and mean energies for the NMR-based structure of integramide A.

number of NOEs	
total	99
intraresidue	32
sequential	46
$i,i+n$, $n=2, 3, 4$	21
mean rmsd[a] from ideality of accepted structures	
bonds [Å]	0.0097
angles [°]	1.13
improper [°]	37.40
NOEs [Å]	0.19
mean energies [kcal mol^{-1}] of accepted structures	
$E_{overall}$	299.1
E_{bond}	23.7
E_{angle}	90.9
E_{NOE}	165.7

[a] Root-mean-square deviation.

Out of the 150 structures that were generated, 100 had violations of the NOE restraints lower than 0.5 Å. The 33 structures with a total energy less than 300 kcal mol^{-1} were selected, and their superposition is shown in Figure 12. All of these structures converge to a well-defined, mixed 3_{10}-/α-helical conformation throughout the sequence, with a backbone average pairwise root-mean-square deviation of (0.26 ± 0.10) Å (Table 3). The lowest-energy 3D structure, shown in Figure 13, exhibits a clear amphipathic character with the three L-Hyp residues at positions 2, 9, and 13 forming the hydrophilic face.

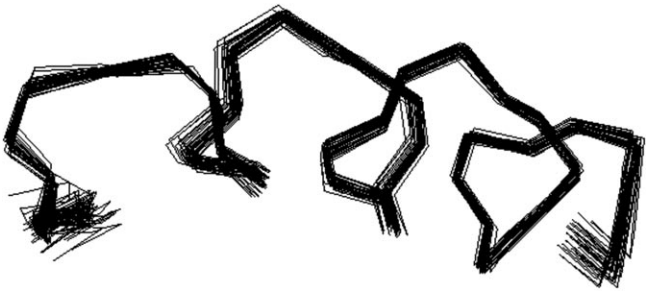

Figure 12. Backbone representation of the 33 structures with energy < 300 kcal mol^{-1} resulting from the MD calculations of integramide A with the backbone atoms superimposed.

Table 3. Average values [°] of torsion angles ϕ_m and ψ_m and the relative standard deviations resulting from the 33 calculated structures (energy < 300 kcal mol^{-1}) of integramide A.

Residue	ϕ_m	$\Delta\phi$	ψ_m	$\Delta\psi$
D-Iva[1]	–	–	−42.6	±0.5
L-Hyp[2]	−84.0	±1.1	3.3	±1.6
L-Ile[3]	−80	±2	−21.4	±1.7
L-Iva[4]	−73.3	±0.9	−27.1	±0.6
L-Leu[5]	−81.5	±1.4	−25.4	±0.8
Aib[6]	−88.3	±0.9	−43.0	±0.7
Aib[7]	−73.5	±0.6	−23.4	±1.4
Aib[8]	−68.3	±1.7	−61.5	±1.1
L-Hyp[9]	−70.6	±0.6	−27	±3
L-Leu[10]	−72.7	±1.9	−29.6	±1.5
L-Iva[11]	−82	±3	−40.4	±1.0
Aib[12]	−34.2	±1.3	−53.1	±0.7
L-Hyp[13]	−72.8	±0.6	−44.3	±1.7
L-Iva[14]	−50.4	±0.8	−22.1	±0.6
D-Iva[15]	−84.1	±2.8	−78.7	±0.7
Gly[16]	−29.6	±1.5	–	–

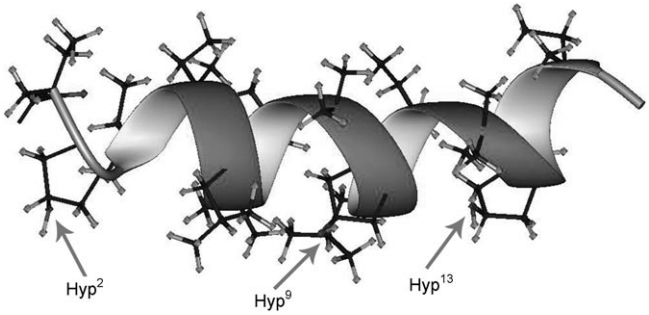

Figure 13. Representation of the 3D structure with the lowest energy obtained for integramide A. The three L-Hyp residues are labeled.

Conclusion

Our interest in the study of integramides originated not only from their intrinsic activity as effective inhibitors of HIV-1 integrase,[4] but also from the observation that their primary structures are closely related to those of peptaibols[23]/peptaibiotics,[7c,24] a class of naturally occurring peptides that are characterized by a high occurrence of the strongly 3_{10}/α-helicogenic, C^α-methylated α-amino acids Aib[16] and Iva.[15]

Although synthetic methods for peptides based on sterically demanding C^α-methylated α-amino acids have been already described,[7] the total syntheses of integramide A, a peptide comprising 16 amino acids, and its D-Iva[14]-L-Iva[15] diastereomer, are notable achievements. Indeed, these compounds present some remarkable challenges due to the sterically hindered nature of multiple amino acids, the acid sensitivity of three tertiary amide bonds, and the propensity of a few N-terminal dipeptides to cyclize, with the related potential loss of two residues from the sequence.

Our very detailed, 3D structural analysis on integramide A and selected short sequences clearly supports the view that the peptide inhibitor has a predominantly 3_{10}-/α-helical structure with amphipathic features under the variety of ex-

perimental conditions used. Notably, in the C-terminal half of the molecule, the Aib(Iva) backbone constraints outweigh the Hyp conformational preference for the *semi*-extended type II poly-(L-Pro)$_n$ conformation. This conclusion agrees well with literature reports on model peptides and on naturally occurring peptaibiotics with repeating Aib(Iva)-L-Pro(Hyp) sequences as well.[25] These compounds are characterized by a β-turn ribbon structure in which the regularity of the 3_{10}-helical backbone ϕ,ψ torsion angles is preserved despite a substantial presence of Pro(Hyp) residues, which is more than compensated for by the extremely strong folding propensity of the preceding Aib(Iva) residues. Remarkably, in a β-turn ribbon segment, the orientation of the peptide carbonyls with respect to the helix axis is not significantly modified compared to that of these same groups in the 3_{10}-helix, but some of these carbonyl groups cannot form hydrogen bonds with the N-alkylated Pro(Hyp) residues. As a result, these C=O groups are available to interact with hydrogen-bonding donor solvents or with other surrounding peptide (protein) molecules.

Several approaches have been used to identify peptides that inhibit HIV-1 integrase.[3] Of particular significance are the conclusions of Roques and co-workers,[3c] who isolated a dodecapeptide inhibitor (EBR28) that binds tightly to the enzyme. An NMR spectroscopic structure analysis showed that under favorable experimental conditions this peptide adopts an α-helical conformation with amphipathic properties. Further evidence suggested that the peptide binds the integrase catalytic core, thus impairing the enzyme dimerization motif that is essential for its activity. Moreover, the hydrophobic face of the α helix seems implicated in this interaction. We believe that the hexadecapeptide main-chain length, the stable helical properties, and the strongly amphipathic nature of integramides might mimic the corresponding characteristics of EBR28 and its proposed mechanism of integrase inhibition. It is also our view that X-ray diffraction analyses of peptide inhibitor–integrase complexes can be extremely useful to elucidate the mechanism of action and optimize drug candidates that target integration of HIV. The low conformational flexibility shown by integramide A, typical of the highly crystalline Aib/Iva-rich peptides,[15,16] will facilitate such analyses.

Experimental Section

Synthesis and characterization of peptides: The strategy of synthesis of the peptides discussed in this work is illustrated in Scheme 1. Characterization details are reported in the Supporting Information.

X-ray diffraction: Single crystals of Z-L-Hyp-L-Iva-D-Iva-Gly-O*t*Bu and Z-L-Iva-L-Leu-(Aib)$_3$-O*t*Bu were grown from ethyl acetate/petroleum ether solution, whereas crystals of Z-L-Ile-L-Iva-L-Leu-(Aib)$_3$-O*t*Bu were grown by slow evaporation from acetonitrile solution. Diffraction data were collected at $T=293(2)$ K with $Cu_{K\alpha}$ radiation ($\lambda=1.54178$ Å) using a Philips PW 1100 diffractometer in the θ–2θ scan mode up to $\theta=60°$. The structures were solved by direct methods with the SIR 2002 program.[26a] Refinements were carried out by least-squares procedures on F^2, using all data, by application of the SHELXL97 program.[26b] All non-hydrogen atoms were refined anisotropically. Hydrogen atoms were calculated at idealized positions and refined using a riding model.

Z-L-Hyp-L-Iva-D-Iva-Gly-OtBu. Formula: $C_{29}H_{44}N_4O_8$; formula weight: 576.7; orthorhombic, space group $P2_12_12_1$; unit cell parameters: $a=9.440(2)$, $b=11.768(2)$, $c=29.962(4)$ Å; $V=3328.5(10)$ Å^3; $Z=4$; $\rho_{calcd}=1.151$ mg m^{-3}; crystal size: $0.40\times0.15\times0.07$ mm^3; data/parameters: 3369/359; $R_1=0.059$ [on $F\geq4\sigma(F)$]; $wR_2=0.176$ (on F^2, all data); goodness of fit on F^2: 0.951; largest peak and hole in the final difference Fourier map: 0.264 and -0.188 e Å^{-3}.

Z-L-Iva-L-Leu-(Aib)$_3$-OtBu. Formula: $C_{35}H_{57}N_5O_8$; formula weight: 675.9; monoclinic, space group $P2_1$; unit cell parameters: $a=10.096(2)$, $b=17.798(3)$, $c=11.554(2)$ Å; $\beta=105.28(5)°$; $V=2002.7(6)$ Å^3; $Z=2$; $\rho_{calcd}=1.121$ mg m^{-3}; crystal size: $0.45\times0.40\times0.10$ mm^3; data/restraints/parameters: 3279/42/430; $R_1=0.141$ [on $F\geq4\sigma(F)$]; $wR_2=0.334$ (on F^2, all data); goodness of fit on F^2: 1.696; largest peak and hole in the final difference Fourier map: 0.530 and -0.630 e Å^{-3}. The C$^\gamma$ atom of the L-Iva residue is disordered and was refined on two sites with population parameters 0.55 and 0.45, respectively.

Z-L-Ile-L-Iva-L-Leu-(Aib)$_3$-OtBu acetonitrile hemisolvate. Formula: $C_{41}H_{68}N_6O_9\times{}^1/_2\ CH_3CN$; formula weight: 809.5; orthorhombic, space group $C222_1$; unit cell parameters: $a=13.580(2)$, $b=19.486(3)$, $c=38.283(4)$ Å; $V=10\,130(2)$ Å^3; $Z=8$; $\rho_{calcd}=1.062$ mg m^{-3}; crystal size: $0.30\times0.20\times0.07$ mm^3; data/restraints/parameters: 4130/44/519; $R_1=0.082$ [on $F\geq4\sigma(F)$]; $wR_2=0.233$ (on F^2, all data); goodness of fit on F^2: 0.926; largest peak and hole in the final difference Fourier map: 0.332 and -0.264 e Å^{-3}. The cocrystallized acetonitrile molecule occupies a ($^1/_2$, *y*, $^1/_4$) special position and shows orientational disorder.

CCDC-726112, 726113, and 726114 contain the supplementary crystallographic data for this paper. These data can be obtained free of charge from The Cambridge Crystallographic Data Centre via www.ccdc.cam.ac.uk/data_request/cif.

Circular dichroism: The CD spectra were obtained on a Jasco (Tokyo, Japan) J-715 spectropolarimeter. Cylindrical fused quartz cells (Hellma) of 0.1 mm path length were used. The values are expressed in terms of $[\Theta]_R$, residue molar ellipticity (deg cm^2 dmol^{-1}). Spectrograde MeOH and TFE (Acros, Geel, Belgium) were used as solvents.

Infrared absorption: The FTIR absorption spectra were recorded by using a Perkin–Elmer 1720 X FTIR spectrophotometer, nitrogen flushed, equipped with a sample-shuttle device, at 2 cm^{-1} nominal resolution, averaging 100 scans. Cells with path lengths of 0.1, 1.0, and 10 mm (with CaF_2 windows) were used. Spectrograde deuterochloroform (99.8% D) was purchased from Aldrich (St. Louis, MO). Solvent (baseline) spectra were recorded under the same conditions.

Chiral liquid chromatography: total hydrolysis:[10] Synthetic L-Iva^{14}-D-Iva^{15} hexadecapeptide or its D-Iva^{14}-L-Iva^{15} diastereomer (0.48 mg) was hydrolyzed in a 6 M aqueous solution of HCl (0.5 mL) for 18 h at 120 °C, and evaporated to dryness. Derivatization: 1 M aqueous solution of $NaHCO_3$ (100 μL) and Marfey's reagent (N$^\alpha$-(2,4-dinitro-5-fluorophenyl)-L-alanine amide, FDNP-L-Ala-NH$_2$, Sigma, St. Louis, MO) (1% in acetone, 100 μL) were added. The mixture was sonicated and incubated at 40 °C for 1 h in a closed vial. A 1 M aqueous solution of HCl (100 μL) and dimethylsulfoxide (200 μL) were added, and aliquots of 5 μL injected into the HPLC column. Instruments: an HP model 1100 apparatus with a quaternary pump (Hewlett–Packard, Waldbronn, Germany) and a photodiode array detector set at 340 nm; LiChroCART Superspher 60 RP-Select B column (250 mm × 4 mm ID; 4 μm particle size; Merck, Darmstadt, Germany). Gradient elution: eluant A: 50 mM triethylammonium phosphate buffer, pH 3.0; eluant B: acetonitrile (100%); gradient: 15% B to 60% B in 75 min; flow rate: 1.2 mL min^{-1}.

Chiral gas chromatography: total hydrolysis: Natural integramide A[4] or the synthetic L-Iva^{14}-D-Iva^{15} hexadecapeptide (0.1 mg) was hydrolyzed in a 6 M aqueous solution of HCl (0.5 mL) for 18 h at 120 °C and evaporated to dryness. Then, HCl in 2-propanol (0.5 mL; generated from a mixture of AcCl/2-propanol 2:8 v/v) was added and the esterification was performed for 1 h at 100 °C in a closed vial. Solvents were removed in a stream of nitrogen, CH_2Cl_2 (250 μL) and trifluoroacetic anhydride (50 μL) were added, and the mixture heated at 100 °C for 20 min. Sol-

vents were removed in a stream of nitrogen, CH_2Cl_2 (200 μL) was added, and 5 μL aliquots were injected into the gas chromatographic (GC) column. Instruments: a GC–MS apparatus, with an A17 GC and a Shimadzu 5000 MS, was used. For chiral analysis of amino acid derivatives, a Chirasil-L-Val capillary column (25 m × 0.35 mm ID; Varian, Darmstadt, Germany) and helium as carrier gas were employed. Solvents and reagents were from Merck.

Mass spectrometry:[10b] For ESI-CID-MS measurements, a calibrated LCQ-MS™ (Thermo Quest, Finnigan MAT, San José, CA) was used. N_2 served as sheath gas and auxiliary gas. He (purity > 99.9990%, Messer-Griesheim, Krefeld, Germany) was used as collision gas. The temperature of the heated capillary was 250°C. Sheath gas and auxiliary gas were set at 40 and 10 relative units, respectively. Ion source CID–MS was performed at 0 and 45% relative collision energies. Sequence analyses were carried out in the positive ionization mode. The m/z values were recorded in the centroid mode and have an accuracy of ±0.5 Da.

NMR spectroscopy: NMR experiments were carried out on a Bruker AVANCE DMX-600 spectrometer. The peptide concentration was 1.45 mM in deuterated [D_2]TFE. The alcohol OH signal was suppressed by presaturation during the relaxation delay. All homonuclear spectra were acquired by collecting 512 experiments, each one consisting of 64 scans and 2K data points. The spin systems of protein amino acid residues were identified by using standard DQF-COSY[27] and CLEAN-TOCSY[28] spectra. In the latter case, the spin-lock pulse sequence was 70 ms long. The assignment of methyl groups belonging to the same Aib residue was obtained by means of 2D ^1H–^{13}C correlation spectra. To optimize the digital resolution in the carbon dimension, HMQC and HMBC spectra were acquired using selective excitation by means of Gaussian-shaped pulses with 1% truncation.[29]

The C_β-selective HMQC spectra with gradient coherence selection[30] were recorded with 224 t_1 increments of 270 scans and 2K points each.[31] A spectral width of 16 ppm centered at 22 ppm in F1 was used, yielding a digital resolution of 2.36 Hz/pt prior to zero filling. HMBC experiments[32] with selective excitation in the carbonyl region were performed by using a long-range coupling constant of 7.5 Hz, a spectral width in $F1$ of 15 ppm centered at 176 ppm, 250 t_1 experiments of 800 scans, and 4K points in $F2$. The digital resolution in F1, prior to zero filling, was 2.2 Hz/pt. NOESY experiments were used for sequence-specific assignment. To avoid the problem of spin diffusion, the buildup curve of the volumes of NOE cross-peaks as a function of mixing time (50 to 500 ms) was determined first (data not shown). The mixing time of the NOESY experiments used for interproton distance determination ranged from 200 to 250 ms, that is, in the linear part of the NOE buildup curve. Interproton distances were obtained by integration of the NOESY spectra using the XEASY[33] package. The calibration was based on the average of the integration values of the cross peaks due to the interactions between the two β-geminal protons of the Leu side-chain residues and the two δ-geminal protons of the Hyp side-chain residues, set to a distance of 1.8 Å. When peaks could not be integrated because of partial overlap, a distance corresponding to the maximum limit of detection of the experiment (4.0 Å) was assigned to the corresponding proton pair.

Distance geometry and MD calculations were carried out using the simulated annealing (SA) protocol of the XPLOR-NIH 2.9.6 program.[34] For distances involving equivalent or nonstereoassigned protons, r^{-6} averaging was used. The MD calculations involved a minimization stage of 100 cycles, followed by SA and refinement stages. The SA consisted of 30 ps of dynamics at 1500 K (10000 cycles, in 3 fs steps) and of 30 ps of cooling from 1500 to 100 K in 50 K decrements (15000 cycles, in 2 fs steps). The SA procedure, in which the weights of NOE and nonbonded terms were gradually increased, was followed by 200 cycles of energy minimization. In the SA refinement stage, the system was cooled from 1000 to 100 K in 50 K decrements (20000 cycles, in 1 fs steps). Finally, the calculations were completed with 200 cycles of energy minimization using a NOE force constant of 50 kcal mol^{-1}. The generated structures were visualized using the MOLMOL[35] (version 2K.2) program.

[1] Y. Goldgur, R. Craigie, G. H. Cohen, T. Fujiwara, T. Yoshinaga, T. Fujishita, H. Sugimoto, T. Endo, H. Murai, D. R. Davies, *Proc. Natl. Acad. Sci. USA* **1999**, *96*, 13040–13043.

[2] a) R. Craigie, *J. Biol. Chem.* **2001**, *276*, 23213–23216; b) S. P. Singh, F. Pelaez, D. J. Hazuda, R. B. Lingham, *Drugs Future* **2005**, *30*, 277–299; c) R. Dayam, R. Gundla, L. Q. Al-Mawsawi, N. Neamati, *Med. Res. Rev.* **2008**, *28*, 118–154; d) T. A. Prikazchikova, A. M. Sychova, Yu. Agapkina, D. A. Alexandrov, M. B. Gottikh, *Russian Chem. Rev.* **2008**, *77*, 421–434.

[3] a) R. A. Puras Lutzke, N. A. Eppens, P. A. Weber, R. A. Houghten, R. H. A. Plasterk, *Proc. Natl. Acad. Sci. USA* **1995**, *92*, 11456–11460; b) R. G. Maroun, D. Krebs, M. Rashani, H. Porumb, C. Auclair, F. Troalen, S. Fermandjian, *Eur. J. Biochem.* **1999**, *260*, 145–155; c) V. R. de Soultrait, A. Caumont, V. Parissi, N. Morellet, M. Ventura, C. Lenoir, S. Litvak, M. Fournier, B. Roques, *J. Mol. Biol.* **2002**, *318*, 45–48; d) L. Zhao, M. K. O'Reilly, M. D. Shultz, J. Chmielewski, *Bioorg. Med. Chem. Lett.* **2003**, *13*, 1175–1177; e) K. Krajewski, C. Marchand, Y.-Q. Long, Y. Pommier, P. P. Roller, *Bioorg. Med. Chem. Lett.* **2004**, *14*, 5595–5598; f) I. Oz Gleenberg, O. Avidan, Y. Goldgur, A. Herschhorn, A. Hizi, *J. Biol. Chem.* **2005**, *280*, 21987–21996; g) H.-Y. Li, Z. Zawahir, L.-D. Song, Y.-Q. Long, N. Neamati, *J. Med. Chem.* **2006**, *49*, 4477–4486; h) P. Cherepanov, A. L. B. Ambrosio, S. Rahman, T. Ellenberger, A. Engelman, *Proc. Natl. Acad. Sci. USA* **2005**, *102*, 17308–17313; i) A. Armon-Omer, A. Levin, Z. Hayouka, K. Butz, F. Hoppe-Seyler, S. Loya, A. Hizi, A. Friedler, A. Loyter, *J. Mol. Biol.* **2008**, *376*, 971–982.

[4] S. B. Singh, K. Herath, Z. Guan, D. L. Zink, A. W. Dombrowski, J. D. Polishook, K. C. Silverman, R. B. Lingham, P. J. Felock, D. J. Hazuda, *Org. Lett.* **2002**, *4*, 1431–1434.

[5] M. De Zotti, F. Formaggio, B. Kaptein, Q. B. Broxterman, P. J. Felock, D. J. Hazuda, S. B. Singh, H. Brückner, C. Toniolo, *ChemBioChem* **2009**, *10*, 87–90.

[6] T. Sonke, B. Kaptein, W. H. J. Boesten, Q. B. Broxterman, H. E. Schoemaker, J. Kamphuis, F. Formaggio, C. Toniolo, F. P. J. T. Rutjes in *Stereoselective Biocatalysis* (Ed.: R. N. Patel), Marcel Dekker, New York, **1999**, pp. 23–58.

[7] a) F. Formaggio, Q. B. Broxterman, C. Toniolo in *Houben-Weyl: Methods of Organic Chemistry, Synthesis of Peptides and Peptidomimetics, Vol. E22c* (Eds.: M. Goodman, A. Felix, L. Moroder, C. Toniolo), Thieme, Stuttgart, **2003**, pp. 292–310; b) H. Brückner, M. Currle in *Second Forum Peptides* (Eds.: A. Aubry, M. Marraud, B. Vitoux), Libbey, London, **1989**, pp. 251–255; c) *Peptaibiotics: Fungal Peptides Containing α-Dialkyl α-Amino Acids* (Eds.: C. Toniolo, H. Brückner), Verlag Helvetica Chimica Acta, Zürich, **2009**.

[8] L. A. Carpino, *J. Am. Chem. Soc.* **1993**, *115*, 4397–4398.

[9] A. Moretto, M. Crisma, F. Formaggio, B. Kaptein, Q. B. Broxterman, T. A. Keiderling, C. Toniolo, *Biopolymers* **2007**, *88*, 233–238.

[10] a) R. Bhushan, H. Brückner, *Amino Acids* **2004**, *27*, 231–247; b) C. Theis, T. Degenkolb, H. Brückner, *Chem. Biodiversity* **2008**, *5*, 2337–2355.

[11] M. Crisma, A. Moretto, M. De Zotti, F. Formaggio, B. Kaptein, Q. B. Broxterman, C. Toniolo, *Biopolymers* **2005**, *80*, 279–293.

[12] a) C. H. Görbitz, *Acta Crystallogr. Sect. B* **1989**, *45*, 390–395; b) C. Ramakrishnan, N. Prasad, *Int. J. Protein Res.* **1971**, *3*, 209–231.

[13] a) C. M. Venkatachalam, *Biopolymers* **1968**, *6*, 1425–1436; b) G. D. Rose, L. M. Gierasch, J. A. Smith, *Adv. Protein Chem.* **1985**, *37*, 1–109.

[14] a) E. Benedetti, A. Bavoso, B. Di Blasio, V. Pavone, C. Pedone, C. Toniolo, G. M. Bonora, *Biopolymers* **1983**, *22*, 305–317; b) K. A. Williams, C. M. Deber, *Biochemistry* **1991**, *30*, 8919–8923; c) A. Yaron, F. Naider, *Crit. Rev. Biochem. Mol. Biol.* **1993**, *28*, 31–81; d) S. J. Eyles, L. M. Gierasch, *J. Mol. Biol.* **2000**, *301*, 737–747.

[15] a) F. Formaggio, M. Crisma, G. M. Bonora, M. Pantano, G. Valle, C. Toniolo, A. Aubry, D. Bayeul, J. Kamphuis, *Pept. Res.* **1995**, *8*, 6–15; b) B. Jaun, M. Tanaka, P. Seiler, F. N. M. Kühnle, C. Braun, D. Seebach, *Liebigs Ann.* **1997**, 1697–1710; c) G. Valle, M. Crisma, C. Toniolo, R. Beisswenger, A. Rieker, G. Jung, *J. Am. Chem. Soc.* **1989**, *111*, 6828–6833; d) R. Bosch, H. Brückner, G. Jung, W. Winter, *Tet-*

rahedron **1982**, *38*, 3579–3583; e) U. Slomczynska, D. D. Beusen, J. Zabrocki, K. Kociolek, A. Redlinski, F. Reusser, W. C. Hutton, M. T. Leplawy, *J. Am. Chem. Soc.* **1992**, *114*, 4095–4106.

[16] a) G. R. Marshall in *Intra-Science Chemistry Reports* (Ed.: N. Kharasch), Gordon and Breach, New York, **1971**, pp. 305–326; b) I. L. Karle, P. Balaram, *Biochemistry* **1990**, *29*, 6747–6756; c) C. Toniolo, M. Crisma, F. Formaggio, C. Peggion, *Biopolymers* **2001**, *60*, 396–419; d) C. Toniolo, *Biopolymers* **1989**, *28*, 247–257; e) C. Toniolo, M. Crisma, G. M. Bonora, E. Benedetti, B. Di Blasio, V. Pavone, C. Pedone, A. Santini, *Biopolymers* **1991**, *31*, 129–138; f) V. Pavone, B. Di Blasio, A. Santini, E. Benedetti, C. Pedone, C. Toniolo, M. Crisma, *J. Mol. Biol.* **1990**, *214*, 633–635.

[17] a) C. Toniolo, E. Benedetti, *Trends Biochem. Sci.* **1991**, *16*, 350–353; b) K. A. Bolin, G. L. Millhauser, *Acc. Chem. Res.* **1999**, *32*, 1027–1033.

[18] a) C. Toniolo, A. Polese, F. Formaggio, M. Crisma, J. Kamphuis, *J. Am. Chem. Soc.* **1996**, *118*, 2744–2745; b) F. Formaggio, M. Crisma, P. Rossi, P. Scrimin, B. Kaptein, Q. B. Broxterman, J. Kamphuis, C. Toniolo, *Chem. Eur. J.* **2000**, *6*, 4498–4504.

[19] M. Goodman, A. S. Verdini, C. Toniolo, W. D. Phillips, F. A. Bovey, *Proc. Natl. Acad. Sci. USA* **1969**, *64*, 444–450.

[20] a) E. S. Pysh, C. Toniolo, *J. Am. Chem. Soc.* **1977**, *99*, 6211–6219; b) S. C. Yasui, T. A. Keiderling, F. Formaggio, G. M. Bonora, C. Toniolo, *J. Am. Chem. Soc.* **1986**, *108*, 4988–4993.

[21] G. Jung, H. Brückner, R. Bosch, W. Winter, H. Schaal, J. Strähle, *Liebigs Ann. Chem.* **1983**, 1096–1106.

[22] M. Bellanda, E. Peggion, R. Bürgi, W. van Gunsteren, S. Mammi, *J. Pept. Res.* **2001**, *57*, 97–106.

[23] a) E. Benedetti, A. Bavoso, B. Di Blasio, V. Pavone, C. Pedone, C. Toniolo, G. M. Bonora, *Proc. Natl. Acad. Sci. USA* **1982**, *79*, 7951–7954; b) H. Brückner, H. Graf, *Experientia* **1983**, *39*, 528–530.

[24] a) H. Duclohier, *Chem. Biodiversity* **2007**, *4*, 1023–1026; b) B. Leitgeb, A. Szekeres, L. Manczinger, C. Vágvölgyi, L. Kredics, *Chem. Biodiversity* **2007**, *4*, 1027–1051; c) T. Degenkolb, J. Kirschbaum, H. Brückner, *Chem. Biodiversity* **2007**, *4*, 1052–1067.

[25] a) I. L. Karle, J. Flippen-Anderson, M. Sukumar, P. Balaram, *Proc. Natl. Acad. Sci. USA* **1987**, *84*, 5087–5091; b) B. Di Blasio, V. Pavone, M. Saviano, A. Lombardi, F. Nastri, C. Pedone, E. Benedetti, M. Crisma, M. Anzolin, C. Toniolo, *J. Am. Chem. Soc.* **1992**, *114*, 6273–6278.

[26] a) M. C. Burla, M. Camalli, B. Carrozzini, G. L. Cascarano, C. Giacovazzo, G. Polidori, R. Spagna, *J. Appl. Crystallogr.* **2003**, *36*, 1103; b) G. M. Sheldrick, *Acta Crystallogr. Sect. A* **2008**, *64*, 112–122.

[27] M. Rance, O. W. Sørensen, G. Bodenhausen, G. Wagner, R. R. Ernst, K. Wüthrich, *Biochem. Biophys. Res. Commun.* **1983**, *117*, 479–485.

[28] a) A. Bax, D. G. Davis, *J. Magn. Reson.* **1985**, *65*, 355–360; b) C. Griesinger, G. Otting, K. Wüthrich, R. R. Ernst, *J. Am. Chem. Soc.* **1988**, *110*, 7870–7872.

[29] a) C. Bauer, R. Freeman, T. Frenkiel, J. Keeler, A. Shaka, *J. Magn. Reson.* **1984**, *58*, 442–457; b) L. Emsley, G. Bodenhausen, *J. Magn. Reson.* **1989**, *82*, 211–221.

[30] A. Bax, R. H. Griffey, B. L. Hawkins, *J. Magn. Reson.* **1983**, *55*, 301–315.

[31] A. Bax, S. Subramanian, *J. Magn. Reson.* **1986**, *67*, 565–569.

[32] A. Bax, M. F. Summers, *J. Am. Chem. Soc.* **1986**, *108*, 2093–2094.

[33] XEASY-ETH Automated Spectroscopy 1.4 (Version 60801000 of the XWindow System), see: C. Bartels, T. Xia, M. Billeter, P. Guntert, K. Wüthrich, *J. Biomol. NMR* **1995**, *6*, 1–10.

[34] C. D. Schwieters, J. J. Kuszewski, N. Tjandra, G. M. Clore, *J. Magn. Reson.* **2003**, *160*, 65–74. Based on X-PLOR 3.851 by A. T. Brunger.

[35] R. Koradi, M. Billeter, K. Wüthrich, *J. Mol. Graphics* **1996**, *14*, 51–55.

Received: April 9, 2009
Revised: October 15, 2009
Published online: November 20, 2009

